Neoplasma 2023; 70(3): 350–360

doi:10.4149/neo_2023_230115N27

A new pathway for the transformation of AML in MDS: APA mechanism regulated by NUDT21 and RUNX1

Shuo LI[1], Fanggang REN[2,3], Xiao-Li LIU[1], Hong-Yu ZHANG[1], Zhi-Fang XU[2,3], Daniel Muteb MUYEY[1], Zhuanzhen ZHENG[3], Yan-Hong TAN[2,3], Xiu-Hua CHEN[2,3], Hong-Wei WANG[1,2,3,*]

[1]Shanxi Medical University, Taiyuan, China; [2]The Key Laboratory of Molecular Diagnosis and Treatment of Hematological Diseases of Shanxi Province, Taiyuan, China; [3]Institute of Hematology, The Second Hospital of Shanxi Medical University, Taiyuan, China

**Correspondence: wanghw68@hotmail.com*

Received January 15, 2023 / Accepted June 6, 2023

We have identified that NUDT21 plays a vital role in MDS transformations, while the transcription factor RUNX1 is essential for normal hematopoiesis, which is a high expression in acute myeloid leukemia (AML) and myelodysplastic syndromes (MDS), and we aim to explore the linkage between the two genes and new pathways for MDS transformation to AML. Prediction of RUNX1 expression levels and its relationship with NUDT21 in AML and MDS patients was performed using bioinformatics techniques and validated in patients. Using lentiviral packaging technology, NUDT21 knockdown and overexpression models were developed in AML and MDS cell lines. These models were validated using quantitative polymerase chain reaction (qPCR) and western blotting. The cell cycle, apoptosis, differentiation, and cytokines were examined by flow cytometry, CCK-8 analyzed proliferation, and the intracellular localization of NUDT21 and RUNX1 was examined by immunofluorescence. mRNA transcriptome sequencing was performed on THP-1, MUTZ-1, and Dapars analyzed SKM-1 cell lines and the sequencing data to observe the knockdown effect of NUDT21 on RUNX1. qPCR and western blot revealed a positive correlation between NUDT21 and RUNX1; both were located in the nucleus. Overexpression of NUDT21 reduced apoptosis, promoted cell proliferation, and possibly increased the invasive ability of cells. It also altered the APA site in the RUNX1 3'-UTRs region. NUDT21 regulates RUNX1 gene expression and promotes AML transformation in MDS through an APA mechanism.

Key words: MDS; AML; NUDT21; RUNX1; APA

The term "myelodysplastic syndromes" (MDS) refers to a group of clonal hematological disorders caused by the clonal expansion of mutant pluripotent hematopoietic progenitor cells. These disorders are distinguished by abnormal cell differentiation, abnormal morphology, hemocytopenia, a variable clinical course, and partial conversion to AML [1, 2]. The presence of a low percentage of primitive granulocytes in the bone marrow of MDS is a feature that can initially differentiate MDS from AML [3]. Despite being treated clinically as two separate diseases, MDS and AML share many of the same genes and functional categories, from clonal hematopoiesis of indeterminate potential (CHIP) to MDS/sAML, raising the possibility that the two diseases may be contiguous. MDS patients have a better prognosis and overall survival compared to AML, and therefore it would be clinically essential to delay or stop the conversion of MDS to AML [4–6].

In mammals, there are three RUNX proteins, RUNX1, RUNX2, and RUNX3 [7, 8]. RUNX proteins have a DNA-binding structural domain at their N-terminus, which consists of a 128 amino acid structural domain [9, 10]. The RUNX1 gene is located in chromosome 21q22 and is associated with all stages of hematopoiesis through its interaction with CBF [11]. The RUNX1 deletion leads to the expansion of hematopoietic stem/progenitor cells whose altered function can lead to the development of leukemia [12]. Meanwhile, RUNX1 mutations can affect one or two alleles, involving the RUNT region that binds to DNA or truncating the more distal protein-acting region. In cytogenetically regular patients, RUNX1 mutations are more likely to occur in older patients, highly expressed, suggesting a poor prognosis [12, 13].

NUDT21 is a highly conserved component of CFIm and is involved in the early steps of eukaryotic pre-mRNA assembly. Normally, NUDT21 and CFIM68 bind specifically as dimers to the two UGUA elements upstream of the poly(A) site, transforming the sequence in the two UGUA elements of the mRNA 3'-UTRs from a linear structure to a ring-like struc-

ture, a ring that protects the polyadenylation signal that lies between the two UGUA elements. This prevents cleavage and polyadenylation-specific factors (CPSF) from binding effectively to the polyadenylation signal, preventing CPSF from cleaving the mRNA at this site [14–17]. Therefore, NUDT21 can promote distal polyadenylate signaling or inhibit proximal polyadenylate signaling. In cases where proximal polyadenylate signaling is retained, mRNAs tend to have longer regions of 3'-UTRs, have stronger cis-elements distally than proximally, and are more conserved [18–21]. Some transcriptional regulators of miRNAs will change when the length or structure of 3'-UTRs is altered, resulting in changes in the regulation of mRNA by these miRNA instability elements. These changes in the regulation of mRNA affect the function of RNA-binding proteins, changing mRNA stability and translation and impacting protein expression, affecting cell phenotype and even tissue and organ function [22–24].

Over 70% of the human genome has multiple variable polyadenylation sites that can be cleaved to produce mRNA transcripts of different lengths, a phenomenon known as alternative polyadenylation (APA) [25–26]. During post-transcriptional modification, the 3'-UTR in mRNA has abundant binding sites for RNA regulatory elements [25]. Various solid tumors are associated with regulating APA mechanisms, but the mechanism of action in MDS is unclear [27–29].

Our previous study found that NUDT21 is involved in the transformation of MDS. While RUNX1 is a key gene in the development of MDS disease, we, therefore, hypothesized that NUDT21 might regulate RUNX1 through the APA mechanism and affect MDS transformation into AML.

Materials and methods

Cell culture. Otto Biotech (Shenzhen, China) provided the human MDS cell line SKM-1, KeyGEN BioTECH (Jiangsu, China) provided the HEK293T cells, and the Blood Laboratory Cell Bank of the Second Hospital of Shanxi Medical University provided the AML cell line K562 and THP-1. K562 and THP-1 cells were cultured in RPMI-1640 (Gibco) and HEK293T cells were cultured in DMEM (Gibco). All media were prepared using 10% fetal bovine serum (BI, IL) and 1% penicillin (SEVEN BIOTECH, Beijing, China) concentrations. All cells were cultured at 37 °C in a 5% CO_2 thermostat incubator (ThermoFisher, USA). All cells were STR-verified and confirmed free of mycoplasma infection.

Plasmid construction and transfection. The shRNA for NUDT21 was designed as shRNA(s86411), and the overexpression plasmid was designed for NUDT21 and purchased from eJin Biologicals (NM_007006) (Shanghai, China). The NUDT21-specific knockdown plasmids and overexpression plasmids were transfected into 293T cells using Lipo8000 (Beyotime, Shanghai, China) in a serum-free double antibody-free DMEM according to the instructions. The 48 h supernatant was collected and filtered through a 0.45 μm membrane to construct stably transfected cell lines. THP-1, SKM-1, and MUTZ-1 cells in logarithmic growth were inoculated into 24-well plates with supernatant and cultured in a standard medium after 24 h. After approximately 72 h, the cells were screened with 4 μg/ml puromycin for 1 week. The cell transfection rate was tested by qRT-PCR and western blot.

RNA extraction and qRT-PCR. Total RNA was extracted using TRIzol (Takara, Japan), and cDNA synthesis was performed using a cDNA synthesis kit (Takara, Japan). Analysis was performed using an ABI 7500 real-time fluorescence PCR instrument (ABI, USA) and SYBR Green Mix reagent (Takara, Japan). Cycling conditions were pre-denaturation at 95 °C for 30 s, 95 °C for 5 s, and 60 °C for 40 s for 40 cycles of amplification. Expression levels were analyzed using the $2^{-\Delta\Delta Ct}$ method. NUDT21 and RUNX1 expression levels were normalized with GAPDH.

To validate the results of transcriptome sequencing, a pair of primers was designed for 50 bases upstream of pPAS of the RUNX1 gene (GGCCACGCGCTACCACACCTACCT-GCCGCCGCCCTACCCCGGCTCGTCGC), representing the short transcript, using the value of ΔΔCt to represent the use of the proximal polyadenylation site.

ΔΔCt = ΔCt (target average) – ΔCt (control average).

Primer sequences: NUDT21-F: AGATTTCAGCG-CATGAGGGAA; NUDT21-R: GCAGCAGTAACACAT-GGGGT; RUNX1-F: TGAGCTGAGAAATGCTACCGC; RUNX1-R: ACTTCGACCGACAAACCTGAG; GAPDH-F: GAAGGTGAAGGTCGGAGTC; GAPDH-R: GAAGATG-GTGATGGGATTTC; proximal PAS-F: CCTCAGGTTT-GTCGGTCGAA; proximal PAS-R: CTTGCGGTGGGTTT-GTGAAG.

Western blot. The RIPA protein lysate was mixed with a protease inhibitor (SEVEN BIOTECH, Beijing, China) according to the manufacturer's instructions. The extracted proteins concentration was tested by a BCA kit (SEVEN BIOTECH, Beijing, China) and denatured and separated by electrophoresis in 4–20% SDS-PAGE gels (SEVEN BIOTECH, Beijing, China). Membranes were transferred using nitrocellulose film, blocked with BSA (Solarbio, Beijing, China); the membrane was washed 3 times with a triple buffer containing Tween 20 buffer and incubated overnight at 4 °C with a specific primary antibody. Then, the membrane was incubated for 1 h with the corresponding horseradish peroxidase (HRP)-labeled secondary antibody. Chemiluminescent reagents were then used to develop the bands. The image was captured by protein simple.

The following antibodies were used in this study: anti-NUDT21 (ab221994; Abcam, Cambridge, UK), anti-RUNX1 (ab240639, Abcam), anti-GAPDH (E-AB-40337, Elabscience), HRP goat anti-IgG (H+L) (RS0002, Immunoway).

Immunofluorescence. Cells were prepared into cell smears (polylysine-fixed slides were purchased from CITO TEST, Jiangsu, China) and fixed with 4% paraformaldehyde

for 15 min. Cell smears were blocked with 1% BSA and then incubated with NUDT21, RUNX1 primary antibody. Nuclear staining was performed using DAPI (Soarbio, Beijing, China). Detection was performed using a LEICA Ami8 laser confocal microscope.

The migration test. Migration experiments were performed using permeable scaffolds and 8.0 μm clear PET membrane (Corning). 2×10^5 cells were resuspended in 200 μl of RPMI-1640 containing 2% fetal bovine serum and inoculated in the upper chamber of a 24-well Transwell plate. After 24 h incubation, the lower chamber was aspirated and mixed, and the number of migrated cells was counted using a Tissue blue stain.

Cell cycle and apoptosis. The cell cycle was analyzed using a kit (Bioss, Beijing, China), and the assay was performed by multicolor flow cytometry. After two PBS rinses and blocking with 95% ethanol overnight at 4 °C, the cells were labeled with a solution of propidium iodide and RNaseA, incubated for 30 min without exposure to light, and then examined by FCM. The data were then analyzed using the Modfit software.

Apoptosis assays were performed using an apoptosis detection kit (Bioss, Beijing, China). The assay was performed by FC 500 flow cytometer (Beckman, USA).

CCK-8 assay. We inoculated cells at a density of 5×10^3 cells/ml into 96-well plates, added 10 μl of CCK-8 solution (SEVEN BIOTECH, Beijing, China) at the same time each day, and then incubated the plates for 2–4 h. This allowed us to determine the proliferative ability of the cells. After incubation, the absorbance was measured at 450 nm by a CYT3MF multifunctional enzyme marker (Bio Tek, USA) for 4 consecutive days.

Cytokines. The supernatant was aspirated and centrifuged to ensure that the supernatant was free of cells and cell debris. 25 μl of cell supernatant and the same volume of buffer, capture microspheres, and detection antibody were added to the flow tube and incubated for 2 h, then 25 μl of fluorescent detection reagent was added and shaken for 0.5 h, washed with washing buffer, and then used for flow cytometry. The microspheres were then washed with wash buffer (using the UNI-MEDICA 7 cytokine kit) and detected using a flow cytometer.

Flow cytometry. To detect the effect of NUDT21 on cell proliferation and differentiation, we selected the cytosolic antigens CD11b (IM2581U, Beckman, USA) and CD117 (C41144, Beckman, USA) for the flow cytometry assay. 1×10^6 cells were incubated in a flow tube with the appropriate flow antibody (Beckman, USA) for 2 h and then incubated on the machine. The instrumentation and analysis software used was as above.

Transcriptome sequencing. The cDNA libraries were sequenced on the Illumina HiSeq X Ten platform. Differential expression analysis was performed using the DESeq (2012) R package. A $p<0.05$, FoldChange >2, or FoldChange <0.5 were used as differential expression thresholds. Systematic clustering was used to assess the differentially expressed genes, and the gene expression patterns were examined using the GO enrichment method and the KEGG pathway enrichment method, respectively. After resequencing by StringTie, the reference genome and known annotated genes were compared using CuffCompare software for gene structure extension and new transcript identification. Selective splicing of differentially regulated transcripts, heterodimers, or exons was analyzed using ASProfile.

Bioinformatics analysis. Comparison of RUNX1 expression levels in AML and MDS patients with normal controls using the GEPIA (http://gepia.cancer-pku.cn/) and GEO (https://www.ncbi.nlm.nih.gov/geo/) databases. The correlation of NUDT21 and RUNX1 expression in AML patients was analyzed using the GEPIA database. The RUNX1 APA locus was predicted using the UCSC database at https://exon.apps.wistar.org/PolyA_DB/v3/index.php.

Statistical analysis. The differences between the normal and experimental groups were tested by t-test using IBM SPSS Statistics 25.0 statistical software and GraphPad Prism 8.3.0 statistical software. For three independent experiments, values are shown as mean ± standard deviation. A p-value <0.05 was considered to be statistically significant. Correlation analysis was performed using the Pearson correlation test. A p-value <0.05 was considered statistically significant ($^*p<0.05$, $^{**}p<0.01$, $^{***}p<0.001$).

Results

Positive correlation between RUNX1 expression and NUDT21 expression. Bioinformatic analysis showed that RUNX1 was expressed higher in MDS and AML patients than in healthy controls (Figure 1A). In the UCSC database, RUNX1 has been reported to have eight APA loci, but three APA loci have not been identified (Figure 1C). And a significant positive correlation between NUDT21 and RUNX1 was predicted by GEPIA (Figure 1B), so we speculate that NUDT21 may regulate RUNX1 to influence the conversion of MDS to AML through the APA mechanism.

We designed a plasmid model of NUDT21 knockdown and overexpression, transfected 293T using the lentiviral packaging technique, and infected AML cell lines K562 and THP-1, as well as the MDS cell line SKM-1 to create a model of cells that stably express NUDT21 knockdown and overexpression. This was done so that we could further verify the correlation between RUNX1 and NUDT21. Both qRTPCR (Figure 2A) and western blot (Figure 2B) verified successful molding.

We found that RUNX1 expression levels were similarly reduced after the knockdown of NUDT21 by qPCR. At the same time, the overexpression of NUDT21 was reversed. Western blot results were consistent with qRT-PCR and also with our predictions. This indicates that the two genes are indeed associated and positively correlated.

Reduced fluorescence intensity of RUNX1 after knockdown of NUDT21. To verify the effect of NUDT21 on the

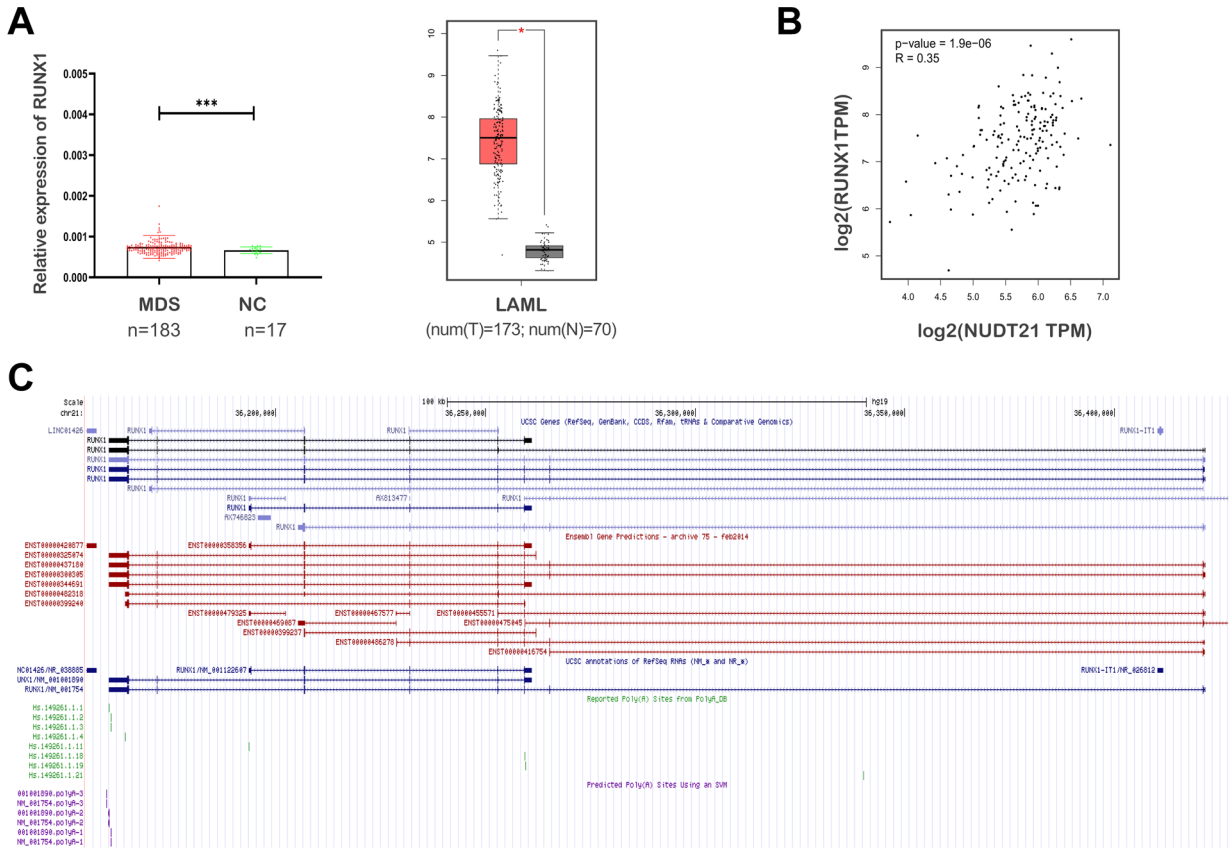

Figure 1. Bioinformatics analysis results. A) Expression levels of RUNX1 are predicted to be higher than normal in both AML and MDS in the database and higher in AML patients. B) NUDT21 expression levels in the UCSC database were positively correlated with RUNX1. C) Multiple APA loci are predicted to be present in the RUNX1 gene in the GEPIA database. *p<0.05, **p<0.01, ***p<0.001

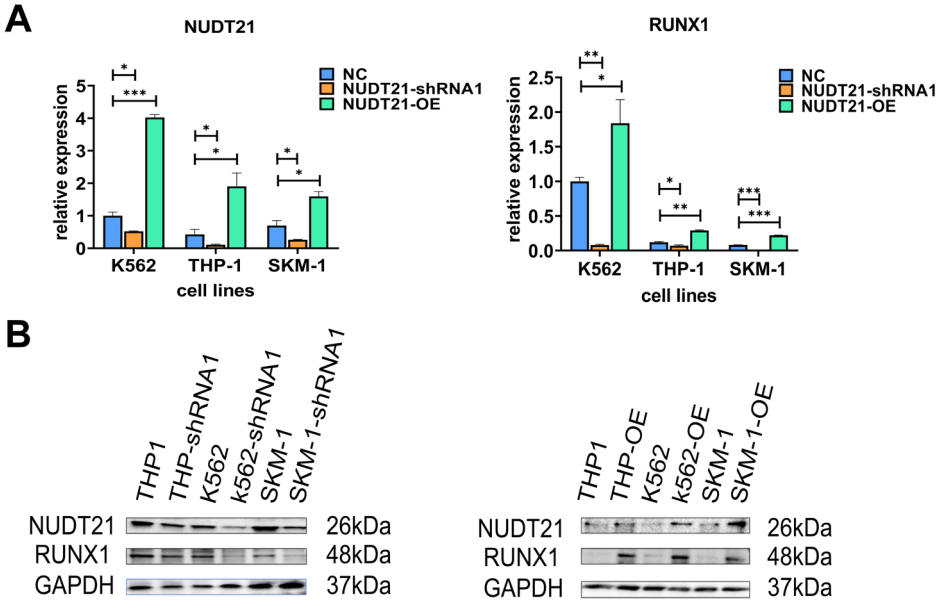

Figure 2. Expression of RUNX1 by qPCR and WB after knockdown and overexpression of NUDT21. A, B) RUNX1 expression levels were reduced after the knockdown of NUDT21, and both RUNX1 expressions were increased after overexpression of NUDT21.

RUNX1 gene and where it functions in the cell, we performed indirect immunofluorescence staining using K562, THP-1, and SKM-1 cells (Figure 3). The results showed that the expression of RUNX1 was also significantly reduced after the knockdown of NUDT21. And both genes were concentrated in the cytoplasm for expression.

Overexpression of NUDT21 can increase migratory cell capacity. We used RPMI-1640 with various serum concentrations in the upper and lower chambers, respectively, to investigate the impact of NUDT21 on cell migration ability (Figure 4A). We inoculated a specific number of cells into the upper chamber with a low serum concentration. Then, we measured the migration ability of cells by counting the number of cells in the lower chamber with a high serum concentration after 24 h. Results demonstrated that NUDT21 overexpression in the THP-1 cell line increased its migratory capacity, whereas NUDT21 knockdown had the opposite effect. In addition, we did not observe significant migration in the K562 and SKM-1 cell lines, and the results were not statistically different.

Overexpression of NUDT21 decreases cell apoptosis and differentiation but increases proliferation. Annexin V as an indicator of apoptosis was utilized on flow cytometry. In the three cell lines, the knockdown of NUDT21 resulted in a significant increase in apoptosis, and the overexpression of NUDT21 led to a decrease in apoptosis (Figure 4B).

In order to determine what effect, the overexpression of NUDT21 has on cells, the proliferation ability of cells was detected by the CCK-8 kit (Figure 4D). The results showed that NUDT21 overexpression significantly increased cell proliferation in K562, THP-1, and SKM-1 cells (Figure 4C). These findings suggest that after overexpressing NUDT21, MDS cells are very prone to proliferate excessively and develop into AML.

CD117, also known as c-kit, is a tyrosine kinase of membrane receptors. CD117 works by binding to stem cell

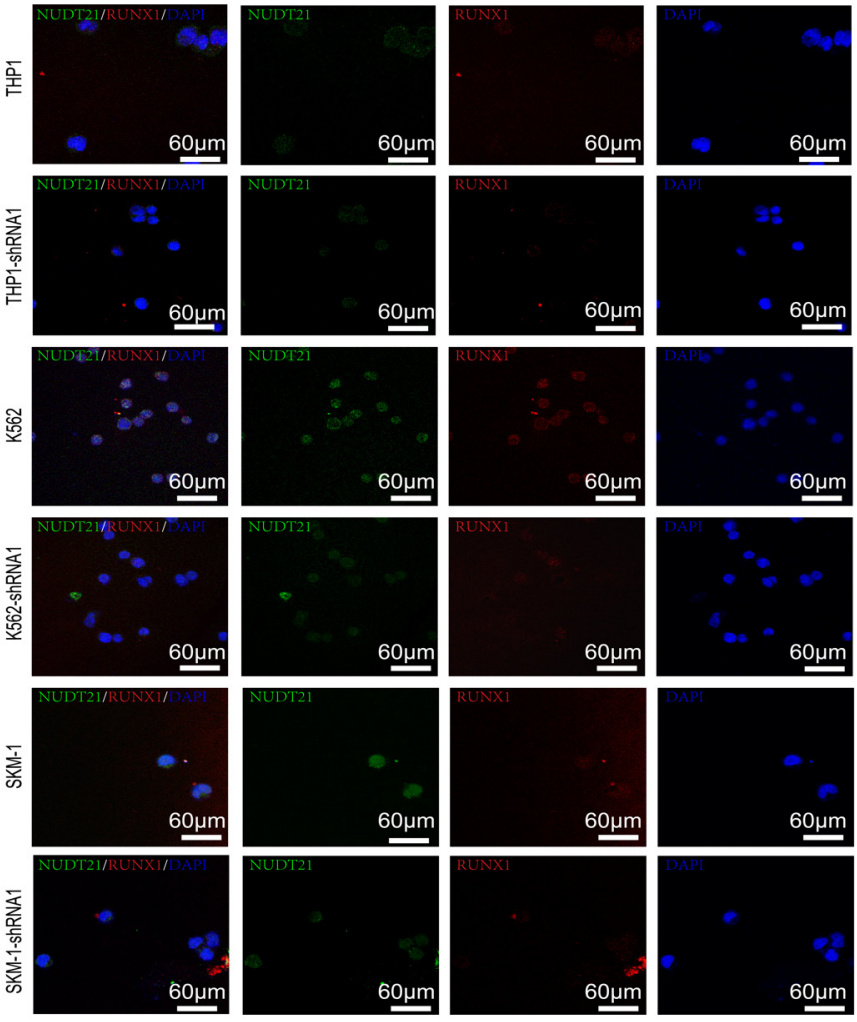

Figure 3. Immunofluorescence test results. After the knockdown of NUDT21, the fluorescence intensity of RUNX1 was reduced in all three cell lines, and both genes were expressed in the cytoplasm.

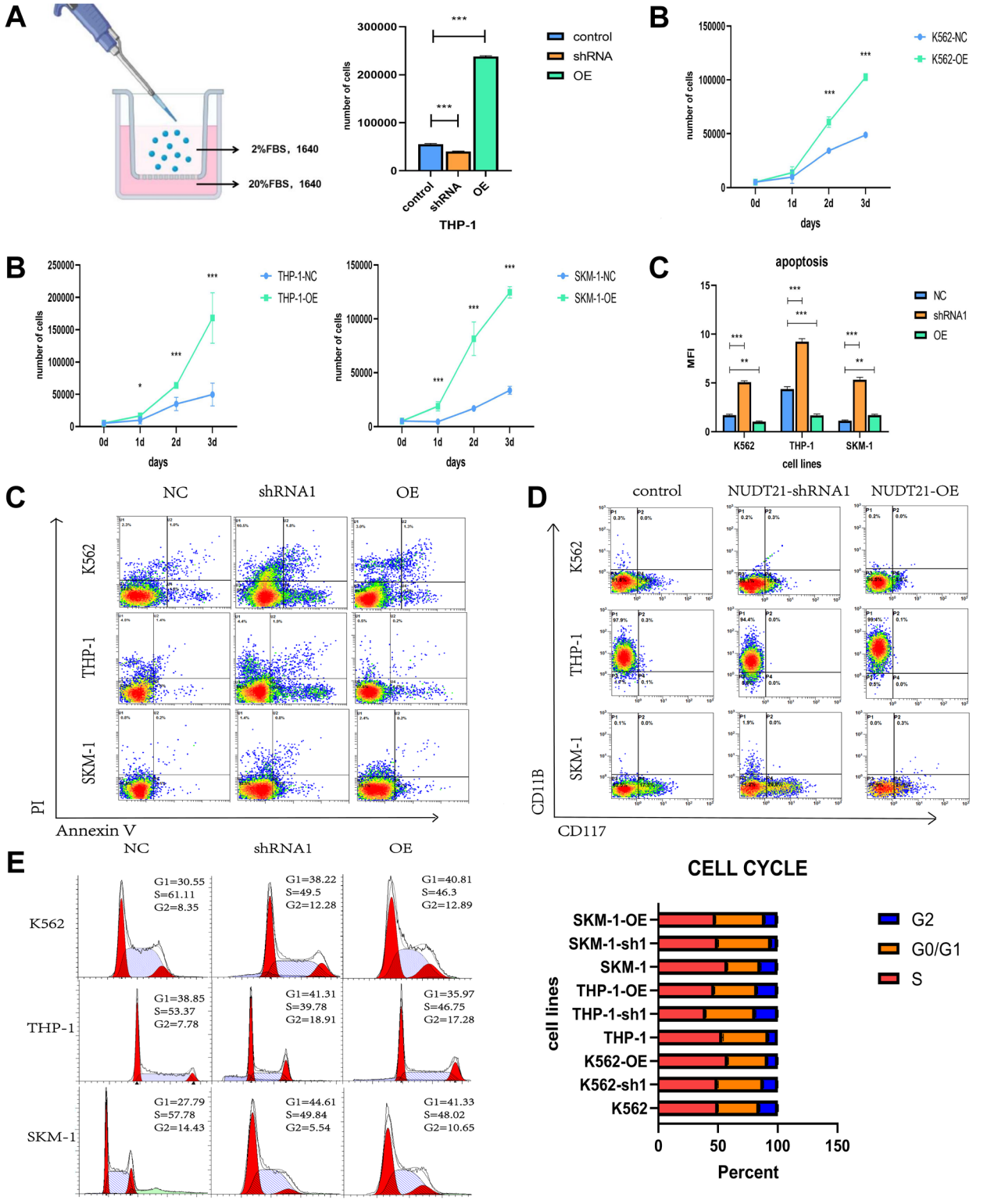

Figure 4. Cell migration assay and flow cytometry for apoptosis, proliferation, and cycle results. A) Sketch of migration assay pattern, THP-1 cell line with diminished migration ability after knockdown of NUDT21 and enhanced migration ability after overexpression of NUDT21. B) The apoptosis of the three cell lines was detected by flow cytometry. The apoptosis of the three cell lines increased after NUDT21 knockdown but reversed after NUDT21 overexpression. C) The proliferation and differentiation of the three cell lines were detected by flow cytometry. D) CCK-8 assay demonstrated that NUDT21 overexpression promoted proliferation in K562, THP-1, and SKM-1 cell lines. E) Cell cycles were detected by flow cytometer.

factors, forming a dimer, and activating tyrosine kinase activity, which drives individual development and balance by influencing signal transduction molecules to regulate cell cycling and differentiation patterns. CD11b is a molecular marker of differentiation; it is often detected together with CD117 to indicate cell proliferation and differentiation. However, our results show no significant change in the groups (Figure 4E).

Knockdown of NUDT21 affects the cell cycle. To verify whether NUDT21 affects the cell cycle, we performed a cycling assay on K562, THP-1, and SKM-1 cells and found that in overexpressing cells, the G1 phase of K562 and THP-1 cells was shortened, and the G1 phase of SKM-1 cells was increased. In knockdown cells, the G1 phase of K562 and THP-1 cells became longer, while the G1 phase of SKM-1 cells remained increased. Combined with the results of proliferation and apoptosis assays, we speculate that this may be related to the ongoing conversion of MDS cells to AML cells.

Knocking down NUDT21 resulted in a shortening of the 3'-UTR of the RUNX1 gene. To investigate the reason for the reduction of RUNX1 after NUDT21 knockdown, we extracted total RNA from THP-1, SKM-1, and their knockdown cell models and performed mRNA transcriptome sequencing, which showed that RUNX1 might contain multiple APA sites (Figure 5A). The sequencing data show that whether NUDT21 is knocked down, the last exon of RUNX1 mRNA has significantly different coverage. The difference may be due to an APA mechanism, which causes the 3'-UTR of pre-mRNA to be cleaved at different positions and add poly(A) sequences. Moreover, the MOTIF plot had multiple sites with very high A content, thus suggesting that RUNX1 may have multiple APA sites, and these loci are associated with NUDT21, which is consistent with the database prediction findings. We also analyzed the related genes affecting the 3'-UTR in the control and knockdown groups, and again RUNX1 affected the length of the 3'-UTR in the knockdown group cells, which showed a shortened 3'-UTR length.

qPCR results showed that the knockdown of NUDT21 in THP-1 and SKM-1 cells led to an increase in ΔΔCt pPAS, indicating an increased usage of the RUNX1 proximal polyadenylation site after the knockdown of NUDT21, further validating the sequencing results (Figure 5B).

Discussion

Splicing, capping, and polyadenylation are the three main steps in mRNA maturation. Polyadenylation is the last key step in mRNA maturation, where the 3' end of pre-mRNA is cleaved, and poly(A) sequences are added, which plays an essential role in the stability of mRNA and its cellular function [30–32]. It is known as alternative cleavage and polyadenylation (APA). It occurs because more than 70% of the human genome has several variable polyadenylation sites that can be cleaved to produce different lengths of mRNA transcripts. The APA can affect RNA localization, stability, translation efficiency, and function and increase the likelihood of disease progression [27, 33].

NUDT21 is a highly conserved component of CFIm involved in the early steps of eukaryotic pre-mRNA assembly [19]. When the length or structure of 3'-UTRs is changed, the function of RNA-binding proteins leads to changes in mRNA stability and translation, and protein expression [34].

We demonstrated the abnormal expression of NUDT21 in AML and MDS patients through databases and clinical samples and found that the expression of RUNX1 decreased with the knockdown of NUDT21 by transcriptome sequencing. Meanwhile, we first performed validation on NUDT21-related cell models to ensure the correlation of NUDT21-RUNX1 expression and showed that both are at the exact location in cells. According to the findings of the proliferation, differentiation, apoptosis, and cell cycle assays, high expression of NUDT21 causes high expression of RUNX1, which interacts with various proteins through its structural domain to alter the normal physiological activities of the cells. This, in turn, enables cancer cells to spread rapidly or can lead to MDS transformation. We, therefore, suggest the existence of NUDT21 influencing MDS to transform AML through the APA mechanism by regulating RUNX1; a model sketch is shown below (Figure 6).

However, some of our results do not fully reflect that NUDT21 affects cells, such as cytokines, which will be the focus of our subsequent study. Interestingly, in our cycle results, we found an increase in G1 phase expression in SKM-1 cells regardless of whether NUDT21 was knocked down or overexpressed, which we speculate is because there is not a single pathway in the transformation of MDS to AML. That knockdown of NUDT21 will likely activate other pathways leading to leukemic cell progression. In addition, we found that apoptosis was not significantly reduced in the three cell lines after overexpression of NUDT21 and that in SKM-1 cells was slightly increased. In this regard, we further performed proliferation assays on the overexpressed cells and found that the overexpressed cells increased their proliferation. Thus, we believe that the increase in cell proliferation following overexpression, which increases the total number of apoptotic cells, is the cause of the lack of a significant reduction in apoptosis in overexpressed cells. As a result, the difference in the proportion of apoptotic cells to the total number of cells is insignificant.

MDS predominates in middle-aged and older people but recent studies have shown a clear trend toward younger age [35, 36]. The specific mechanism of MDS transformation into AML is not yet uniformly established, and most current studies have focused on gene mutations and epigenetic modifications [37]. In recent years, various studies have demonstrated that APA mechanisms are key to the development of multiple types of cancers, and NUDT21,

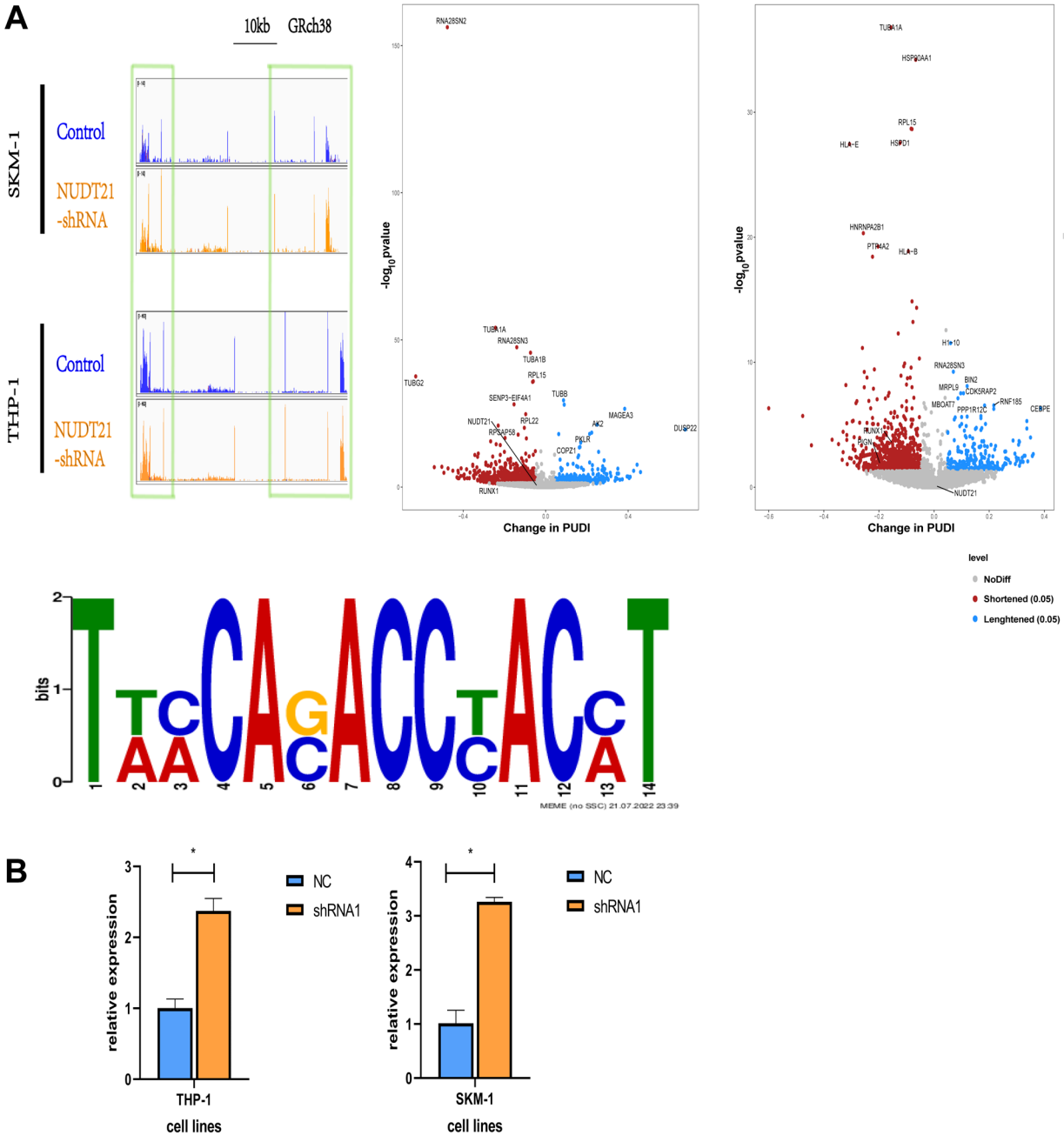

Figure 5. mRNA transcriptome sequencing results. Transcriptome sequencing and differential gene analysis. Sequencing results from Dapars analysis showed that the APA locus was altered after the knockdown of NUDT21, and the 3'-UTR of the RUNX1 gene was shortened (A). qPCR results show increased usage of the RUNX1 proximal polyadenylation site after the knockdown of NUDT21 (B).

a key component of APA, also plays a pivotal role in the process of MDS transformation [5, 38]. Perhaps designing targeted drugs against NUDT21 in MDS patients to restore its expression, allowing mRNA transcripts to be cleaved at their regular sites, and restoring normal cell physiology is a novel therapeutic approach [20, 39]. The study of NUDT21 and APA mechanisms aims to provide new ideas and directions for developing targeted drugs to reduce the risk of their transformation into AML.

In conclusion, this study suggests that NUDT21 has a role in transforming MDS into AML through the regulation of RUNX1 by the APA mechanism, which improves our understanding of the transformation of MDS disease and provides new targets and ideas for future MDS therapy.

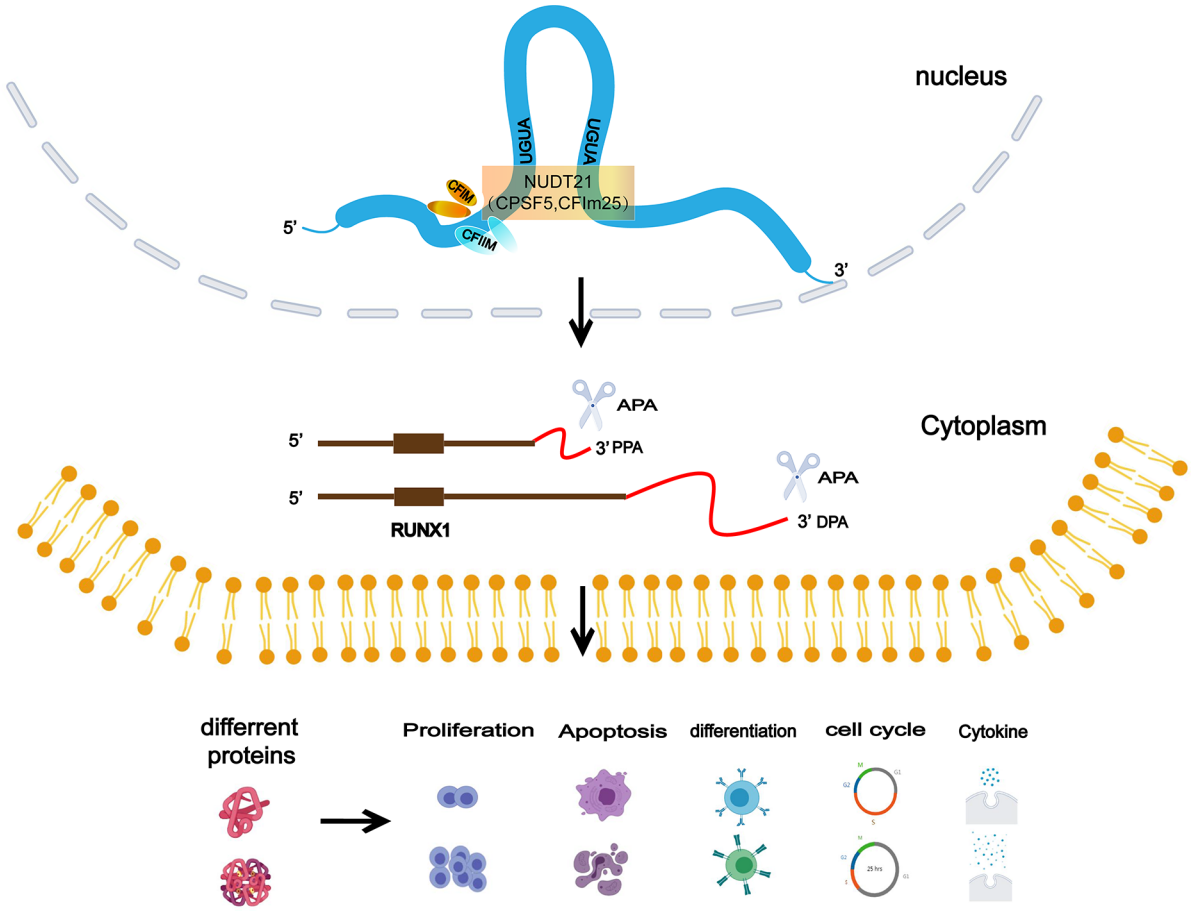

Figure 6. Sketch of the APA mechanism of action. NUDT21 abnormalizes the RUNX1 gene by regulating mRNA 3'-UTR length and alters normal cell function through differentiation, apoptosis, differentiation, cycling, cytokines, etc., and MDS transformation occurs.

Acknowledgments: This work was supported by the National Natural Science Foundation of China (NO. NO.81670126;81500104), The Shanxi Natural Science Foundation of China (NO.201801D1110; NO.201801D22140903), Graduate Innovation Fund of Shanxi Province. The Second Hospital of Shanxi Medical University Doctoral Fund Project (202201-2), the Second Hospital of Shanxi Medical University Scientific and Technological Activities of Overseas Students Merit Grant Project (2020041), the Second Hospital of Shanxi Medical University Scientific Research Grant Project for Returned Overseas Students (2021-171), the Special Project of Wu Jieping Medical Foundation (320.6750.2022-8-4), the Second Hospital of Shanxi Medical University Youth Fund Project (201708).

References

[1] ARBER DA, ORAZI A, HASSERJIAN R, THIELE J, BOROWITZ MJ et al. The 2016 revision to the World Health Organization classification of myeloid neoplasms and acute leukemia. Blood 2016; 127: 2391–2405. https://doi.org/10.1182/blood-2016-03-643544

[2] CHEN BY, SONG J, HU CL, CHEN SB, ZHANG Q et al. SETD2 deficiency accelerates MDS-associated leukemogenesis via S100a9 in NHD13 mice and predicts poor prognosis in MDS. Blood 2020; 135: 2271–2285. https://doi.org/10.1182/blood.2019001963

[3] HOSPITAL MA, VEY N. Myelodysplastic Syndromes: How to Recognize Risk and Avoid Acute Myeloid Leukemia Transformation. Curr Oncol Rep 2020; 22: 4. https://doi.org/10.1007/s11912-020-0869-0

[4] MENSSEN AJ, WALTER MJ. Genetics of progression from MDS to secondary leukemia. Blood 2020; 136: 50–60. https://doi.org/10.1182/blood.2019000942

[5] SHIOZAWA Y, MALCOVATI L, GALLÌ A, PELLAGATTI A, KARIMI M et al. Gene expression and risk of leukemic transformation in myelodysplasia. Blood 2017; 130: 2642–2653. https://doi.org/10.1182/blood-2017-05-783050

[6] SPERLING A, GIBSON CJ, EBERT BL. The genetics of myelodysplastic syndrome: from clonal haematopoiesis to secondary leukaemia. Nat Rev Cancer 2017; 17: 5–19. https://doi.org/10.1038/nrc.2016.112

[7] ICHIKAWA M, YOSHIMI A, NAKAGAWA M, NISHIMOTO N, WATANABE-OKOCHI N et al. A role for RUNX1 in hematopoiesis and myeloid leukemia. Int J Hematol 2013; 97: 726–734. https://doi.org/10.1007/s12185-013-1347-3

[8] YOKOTA A, HUO L, LAN F, WU J, HUANG G. The Clinical, Molecular, and Mechanistic Basis of RUNX1 Mutations Identified in Hematological Malignancies. Mol Cells 2020; 43: 145–152. https://doi.org/10.14348/molcells.2019.0252

[9] CHEN CY, LIN LI, TANG JL, KO BS, TSAY W et al. RUNX1 gene mutation in primary myelodysplastic syndrome--the mutation can be detected early at diagnosis or acquired during disease progression and is associated with poor outcome. Br J Haematol 2007; 139(3): 405–414. https://doi.org/10.1111/j.1365-2141.2007.06811.x

[10] GROARKE EM, PATEL BA, SHALHOUB R, GUTIERREZ-RODRIGUES F, DESAI P et al. Predictors of clonal evolution and myeloid neoplasia following immunosuppressive therapy in severe aplastic anemia. Leukemia 2022; 36: 2328–2337. https://doi.org/10.1038/s41375-022-01636-8

[11] WU K, NIE B, LI L, YANG X, YANG J et al. Bioinformatics analysis of high frequency mutations in myelodysplastic syndrome-related patients. Ann Transl Med 2021; 9: 1491. https://doi.org/10.21037/atm-21-4094

[12] KAISRLIKOVA M, VESELA J, KUNDRAT D, VOTAVOVA H, DOSTALOVA MERKEROVA M et al. RUNX1 mutations contribute to the progression of MDS due to disruption of antitumor cellular defense: a study on patients with lower-risk MDS. Leukemia 2022; 36: 1898–1906. https://doi.org/10.1038/s41375-022-01584-3

[13] SIMON L, SPINELLA JF, YAO CY, LAVALLÉE VP, BOIVIN I et al. High frequency of germline RUNX1 mutations in patients with RUNX1-mutated AML. Blood 2020; 135: 1882–1886. https://doi.org/10.1182/blood.2019003357

[14] ALCOTT CE, YALAMANCHILI HK, JI P, VAN DER HEIJDEN ME, SALTZMAN A et al. Partial loss of CFIm25 causes learning deficits and aberrant neuronal alternative polyadenylation. Elife 2020; 9: e50895. https://doi.org/10.7554/eLife.50895

[15] BRUMBAUGH J, DI STEFANO B, WANG X, BORKENT M, FOROUZMAND E et al. Nudt21 Controls Cell Fate by Connecting Alternative Polyadenylation to Chromatin Signaling. Cell 2018; 172: 106–120.e21. https://doi.org/10.1016/j.cell.2017.11.023

[16] BURRI D, ZAVOLAN M. Shortening of 3' UTRs in most cell types composing tumor tissues implicates alternative polyadenylation in protein metabolism. RNA 2021; 27: 1459–1470. https://doi.org/10.1261/rna.078886.121

[17] DHARMALINGAM P, MAHALINGAM R, YALAMANCHILI HK, WENG T, KARMOUTY-QUINTANA H et al. Emerging roles of alternative cleavage and polyadenylation (APA) in human disease. J Cell Physiol 2022; 237: 149–160. https://doi.org/10.1002/jcp.30549

[18] GARAULET DL, ZHANG B, WEI L, LI E, LAI EC. miRNAs and Neural Alternative Polyadenylation Specify the Virgin Behavioral State. Dev Cell 2020; 54: 410–423.e4. https://doi.org/10.1016/j.devcel.2020.06.004

[19] GRUBER AJ, ZAVOLAN M. Alternative cleavage and polyadenylation in health and disease. Nat Rev Genet 2019; 20: 599–614. https://doi.org/10.1038/s41576-019-0145-z

[20] JAFARI NAJAF ABADI MH, SHAFABAKHSH R, ASEMI Z, MIRZAEI HR, SAHEBNASAGH R et al. CFIm25 and alternative polyadenylation: Conflicting roles in cancer. Cancer Lett 2019; 459: 112–121. https://doi.org/10.1016/j.canlet.2019.114430

[21] KUBO T, WADA T, YAMAGUCHI Y, SHIMIZU A, HANDA H. Knock-down of 25 kDa subunit of cleavage factor Im in Hela cells alters alternative polyadenylation within 3'-UTRs. Nucleic Acids Res 2006; 34: 6264–6271. https://doi.org/10.1093/nar/gkl794

[22] LEE SH, SINGH I, TISDALE S, ABDEL-WAHAB O, LESLIE CS et al. Widespread intronic polyadenylation inactivates tumour suppressor genes in leukaemia. Nature 2018; 561: 127–131. https://doi.org/10.1038/s41586-018-0465-8

[23] MASAMHA CP, XIA Z, YANG J, ALBRECHT TR, LI M et al. CFIm25 links alternative polyadenylation to glioblastoma tumour suppression. Nature 2014; 510: 412–416. https://doi.org/10.1038/nature13261

[24] RAN Y, HUANG S, SHI J, FENG Q, DENG Y et al. CFIm25 regulates human stem cell function independently of its role in mRNA alternative polyadenylation. RNA Biol 2022; 19: 686–702. https://doi.org/10.1080/15476286.2022.2071025

[25] SOMMERKAMP P, TRUMPP A. Driving differentiation: targeting APA in AML. Blood 2022; 139: 317–319. https://doi.org/10.1182/blood.2021013814

[26] SUBRAMANIAN A, HALL M, HOU H, MUFTEEV M, YU B et al. Alternative polyadenylation is a determinant of oncogenic Ras function. Sci Adv 2021; 7: eabh0562. https://doi.org/10.1126/sciadv.abh0562

[27] TIAN B, MANLEY JL. Alternative polyadenylation of mRNA precursors. Nat Rev Mol Cell Biol 2017; 18: 18–30. https://doi.org/10.1038/nrm.2016.116

[28] XIANG Y, YE Y, LOU Y, YANG Y, CAI C et al. Comprehensive Characterization of Alternative Polyadenylation in Human Cancer. J Natl Cancer Inst 2018; 110: 379–389. https://doi.org/10.1093/jnci/djx223

[29] XING Y, CHEN L, GU H, YANG C, ZHAO J et al. Downregulation of NUDT21 contributes to cervical cancer progression through alternative polyadenylation. Oncogene 2021; 40: 2051–2064. https://doi.org/10.1038/s41388-021-01693-w

[30] XIONG M, CHEN L, ZHOU L, DING Y, KAZOBINKA G et al. NUDT21 inhibits bladder cancer progression through ANXA2 and LIMK2 by alternative polyadenylation. Theranostics 2019; 9: 7156–7167. https://doi.org/10.7150/thno.36030

[31] ZHANG L, ZHANG W. Knockdown of NUDT21 inhibits proliferation and promotes apoptosis of human K562 leukemia cells through ERK pathway. Cancer Manag Res 2018; 10: 4311–4323. https://doi.org/10.2147/CMAR.S173496

[32] RICHARD S, GROSS L, FISCHER J, BENDALAK K, ZIV T et al. Numerous Post-translational Modifications of RNA Polymerase II Subunit Rpb4/7 Link Transcription to Post-transcriptional Mechanisms. Cell Rep 2021; 34: 108578. https://doi.org/10.1016/j.celrep.2020.108578

[33] XU Z, PLATIG J, LEE S, BOUEIZ A, CHASE R et al. Cigarette smoking-associated isoform switching and 3' UTR lengthening via alternative polyadenylation. Genomics 2021; 113: 4184–4195. https://doi.org/10.1016/j.ygeno.2021.11.004

[34] REN F, ZHANG N, ZHANG L, MILLER E, PU JJ. Alternative Polyadenylation: a new frontier in post transcriptional regulation. Biomark Res 2020; 8: 67. https://doi.org/10.1186/s40364-020-00249-6

[35] TANAKA TN, BEJAR R. MDS overlap disorders and diagnostic boundaries. Blood 2019; 133: 1086–1095. https://doi.org/10.1182/blood-2018-10-844670

[36] GHOBRIAL IM, DETAPPE A, ANDERSON KC, STEENSMA DP. The bone-marrow niche in MDS and MGUS: implications for AML and MM. Nat Rev Clin Oncol 2018; 15: 219–233. https://doi.org/10.1038/nrclinonc.2017.197

[37] HERON M, DOVERN E, BAKKER-JONGES LE, POSTHUMA EFM, BROUWER RE et al. Translating the MDS flow cytometric score into clinical practice. Cytometry B Clin Cytom 2015; 88: 207–209. https://doi.org/10.1002/cyto.b.21208

[38] XU YF, LI YQ, LIU N, HE QM, TANG XR et al. Differential genome-wide profiling of alternative polyadenylation sites in nasopharyngeal carcinoma by high-throughput sequencing. J Biomed Sci 2018; 25: 74. https://doi.org/10.1186/s12929-018-0477-6

[39] FU Y, SUN Y, LI Y, LI J, RAO X et al. Differential genome-wide profiling of tandem 3' UTRs among human breast cancer and normal cells by high-throughput sequencing. Genome Res 2011; 21: 741–747. https://doi.org/10.1101/gr.115295.110